Chemical Science

ROYAL SOCIETY OF CHEMISTRY

EDGE ARTICLE

View Article Online
View Journal | View Issue

Cite this: *Chem. Sci.*, 2024, **15**, 3687

All publication charges for this article have been paid for by the Royal Society of Chemistry

Received 28th November 2023
Accepted 25th January 2024

DOI: 10.1039/d3sc06383f

rsc.li/chemical-science

Photo- and halochromism of spiropyran-based main-chain polymers†

Linh Duy Thai, [abc] Jochen A. Kammerer, [ab] Hatice Mutlu *[d] and Christopher Barner-Kowollik *[abc]

Advanced functional polymeric materials based on spiropyrans (SPs) feature multi-stimuli responsive characteristics, such as a change in color with exposure to light (photochromism) or acids (halochromism). The inclusion of stimuli-responsive molecules in general – and SPs in particular – as main-chain repeating units is a scarcely explored macromolecular architecture compared to side chain responsive polymers. Herein, we establish the effects of substitution patterns on SPs within a homopolymer main-chain synthesized *via* head-to-tail Acyclic Diene METathesis (ADMET) polymerization. We unambiguously demonstrate that varying the location of the ester group (–OCOR) on the chromophore, which is essential to incorporate the SPs in the polymer backbone, determines the photo- and halochromism of the resulting polymers. While one polymer shows effective photochromism and resistance towards acids, the opposite – weak photochromism and effective response to acid – is observed for an isomeric polymer, simply by changing the position of the ester-linker relative to the benzopyran oxygen on the chromene unit. Our strategy represents a simple approach to manipulate the stimuli-response of main-chain SP bearing polymers and highlights the critical importance of isomeric molecular constitution on main-chain stimuli-sensitive polymers as emerging materials.

Introduction

Spiropyrans (SPs), typically containing a benzopyran (chromene) covalently connected to a heterocyclic moiety *via* the spiro-carbon (Fig. 1), constitute a well-known and extensively studied class of multi-stimuli-responsive chemical structures.[1–3] The ring-closed structure of SPs is typically the thermodynamically stable isomer, which can reversibly transform to the ring-opened form upon exposure to various stimuli, such as light irradiation, pH or mechanical force.[1,2,4] The stimuli-responsive SP transformation is accompanied by a vivid color change (*i.e.*, colorless to colored or *vice versa*) and a large polarity difference (*i.e.*, apolar (hydrophobic) to polar/zwitterionic/merocyanine (hydrophilic) form or *vice versa*). Since the first report of synthetic spiropyrans at the beginning of the 20th century,[5] chemists have integrated SPs into polymers, harnessing their responsive properties to generate advanced dynamic functional materials.[3,6,7] Exemplary applications are smart coatings,[8,9] pH/metal ion or force sensors,[10–13] drug delivery,[14] lithography[15,16] or shape-changing materials.[17]

Most stimuli-responsive moieties are tethered directly to the polymer chain as either pendant groups – or to a far lesser extent – as main-chain active groups *via* ester and amide bonds.[18–22] In the realm of SPs, the type of the substituents decorating the SPs, *e.g.*, electron-withdrawing or electron-donating, has a potentially significant influence on the stimuli-sensitiveness of SPs-based polymers.[23–25] However, the impact of ester groups located at different sites of SPs' aromatic moieties (regioisomers) has not been investigated. In fact – to our best knowledge – only two studies explore substituent location variations of the polymerizable group on the benzopyran moiety, leading to different levels of stretching-induced ring-opening and isomerization of the covalently embedded SP units.[11,26] However, the SPs-based monomers were designed such that the SP moiety and the ester group of polymerizable handles were connected *via* a methylene group (–CH_2–) to the chromene moiety.[11,26] Critically, the effect of these designs on the resulting photo- and pH-responsive properties was not explored. Interestingly, nitro-substituted SPs (NO_2-SPs) have frequently been explored, most likely due to the resulting red-shifted electronic absorption and an enhanced quantum efficiency induced by the electron-withdrawing group.[27,28]

[a]*School of Chemistry and Physics, Queensland University of Technology (QUT), 2 George Street, Brisbane, QLD 4000, Australia. E-mail: christopher.barnerkowollik@qut.edu.au*

[b]*Centre for Materials Science, Queensland University of Technology (QUT), 2 George Street, Brisbane, QLD 4000, Australia*

[c]*Institute of Nanotechnology (INT), Karlsruhe Institute of Technology (KIT), Hermann-von-Helmholtz-Platz 1, 76344 Eggenstein-Leopoldshafen, Germany*

[d]*Institut de Science des Matériaux de Mulhouse, UMR 7361 CNRS/Université de Haute Alsace, 15 Rue Jean Starcky, Mulhouse Cedex, 68057, France. E-mail: hatice.mutlu@uha.fr*

† Electronic supplementary information (ESI) available. See DOI: https://doi.org/10.1039/d3sc06383f

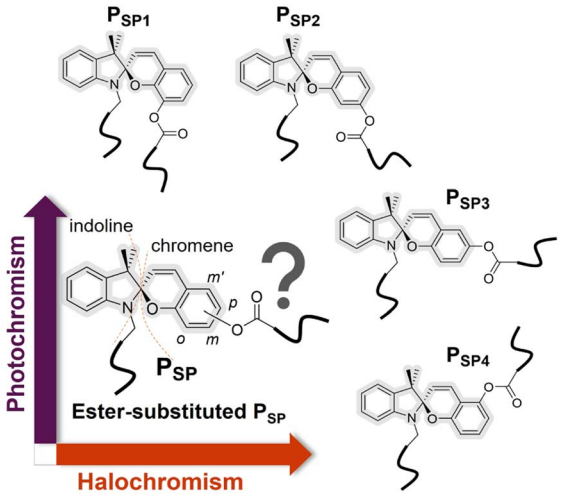

Fig. 1 General structures of four main-chain polymers derived from four regioisomers of a spiropyran scaffold. The sole difference among these regioisomers is the relative position (with respect to the benzopyran oxygen) of the ester group (–OCOR) on the chromene moiety of the spiropyran. We demonstrate dramatic effects of these minor difference on the photo- and halochromism of the resulting polymers. Note that the covalent connection to the chromene moiety can be realized through the carbonyl carbon (–COOR), which is critically different from our design.

Remarkably, in the current literature, the electrochemical contribution of other groups, *e.g.*, esters, is often ignored. However, tuning the properties of responsive macromolecular materials *via* subtle alterations of their chemical structures is undoubtedly a powerful avenue to establish varied property profiles with synthetic ease. Herein, we demonstrate such structural variations and their effect on the resulting material properties, opening a facile route to an advanced class of SP-containing responsive polymer systems.

Main-chain SP-based polymers possess – just as their well-explored side chain equivalents – photo and pH- responsiveness, yet offer additional exclusive qualities, such as mechanochromism[11] and potentially larger motion change[29,30] upon the ring-opening of SPs. Synthetically, however, just a limited number of methods, *e.g.*, Ring-Opening (Metathesis) Polymerization (ROP[26]/ROMP[31]) or Suzuki polycondensation,[32] were employed to install SP moieties into the polymer backbone.[13,33] Here, we employ head-to-tail Acyclic Diene METathesis (ADMET) polymerization to construct SP main-chain polymers.

We thus introduce the synthesis of four main-chain polymers ($\mathbf{P_{SP1}}$, $\mathbf{P_{SP2}}$, $\mathbf{P_{SP3}}$ and $\mathbf{P_{SP4}}$) derived from four regioisomers of SPs *via* ADMET polymerization and investigate their photo- and acid-responsive properties. These polymers differ only in the substitution location on the SP's benzopyran (chromene) moiety (*o*-, *m*-, *p*- and *m*′- position, corresponding to $\mathbf{P_{SP1}}$, $\mathbf{P_{SP2}}$, $\mathbf{P_{SP3}}$ and $\mathbf{P_{SP4}}$, respectively, refer to Fig. 1 and 2) of the ester group (–**O**COR, where R contains a polymerizable handle, inserting the chromophore into the polymer main chain). Note that the benzopyran ring is substituted with the ester oxygen (–**O**COR) rather than the carbonyl carbon (–COOR) of the ester group reported elsewhere for small structures.[34] To our best knowledge, we report SPs bearing an ester group (–**O**COR) substituted at either the *m* or *m*′ position (refer to Fig. 1 and 2) for the first time. The synthetic accessibility of all four substitution sites allows us to systematically study the influence of regio-isomers on the stimuli response of SPs. Interestingly, our results show that such minor structural differences have dramatic effects on the solution photo- and acid-responsiveness of the SP moieties of these polymers. Particularly, while $\mathbf{P_{SP1}}$ is relatively photo-inactive yet acid sensitive, the complete opposite behavior is observed for $\mathbf{P_{SP4}}$. $\mathbf{P_{SP2}}$ responds rapidly to acids (*i.e.*, CF_3COOH and CH_3SO_3H), followed by $\mathbf{P_{SP1}}$ and $\mathbf{P_{SP3}}$.

Results and discussion

Synthesis

Initially, we designed four ADMET monomers, containing four spiropyran regioisomers as main-chain moieties. The handle containing the acrylate group is placed at the indoline nitrogen, while the phenyl ring of the chromene moiety is substituted with an ester group containing the olefin handle at one of the four sites, *o*-, *m*-, *p*- and *m*′-, yielding monomer $\mathbf{M_{SP1}}$, $\mathbf{M_{SP2}}$, $\mathbf{M_{SP3}}$ and $\mathbf{M_{SP4}}$, respectively (Fig. 2). The selective cross-metathesis using a Hoveyda–Grubbs 2nd generation catalyst (HG-II) between the acrylate and olefin functional groups affords the main-chain polymer $\mathbf{P_{SP1}}$, $\mathbf{P_{SP2}}$, $\mathbf{P_{SP3}}$ and $\mathbf{P_{SP4}}$ from the respective monomers (refer to the ESI for full synthesis protocol and characterization of monomers and polymers, Section 2 and 9†). The sectional ^{1}H NMR spectra in Fig. 2 unambiguously evidence the formation of the internal acrylate bond (proton resonances at $\delta \approx 5.75$ and 6.92 ppm) from the cross-metathesis, while leaving the SP chromophores chemically intact. The apparent number-average molar mass (M_n) of these polymers falls in the range of (7500–22 000) g mol^{-1} (Fig. 2, bottom and Table 1), in line with other stimuli-responsive polymers synthesized *via* ADMET polymerization.[35,36] Interestingly, during the polymerization, we observed gelation of the reaction mixture of $\mathbf{M_{SP2}}$ when dichloromethane (DCM) was used as solvent. Gelation was prevented by using 1,2-dichlorobenzene (DCB) as solvent instead, successfully obtaining polymer $\mathbf{P_{SP2}}$ (Fig. 2B). Although the mechanism for the gelation of $\mathbf{M_{SP2}}$ in DCM solution is unclear, we speculate that the general structure of $\mathbf{M_{SP2}}$ with the ester group at the *m*-position of the benzopyran ring (Fig. 2) might allow for a ligand-exchange reaction with the Ru-based HG-II catalyst which could gradually decompose in DCM solvent.[37] On the basis of the observed molar masses (M_n) of the four polymers (Table 1), the acrylate and the olefin handles in $\mathbf{P_{SP3}}$ are in an optimal orientation, enabling rapid polymerization and affording relatively high M_n compared to the other three isomeric polymers. The substitution-site dependence of M_n in ADMET polymerization is also observed in hydrazone-based main-chain polymers.[38]

With regard to the optical properties of the four polymers, there is an insignificant difference in terms of the peak absorption band (λ_{max}) in DCM, corresponding to the π–π^* transition of the chromene moiety, close to the values reported for halogen- and ether-substituted SPs (λ_{max} = (297–299) nm,

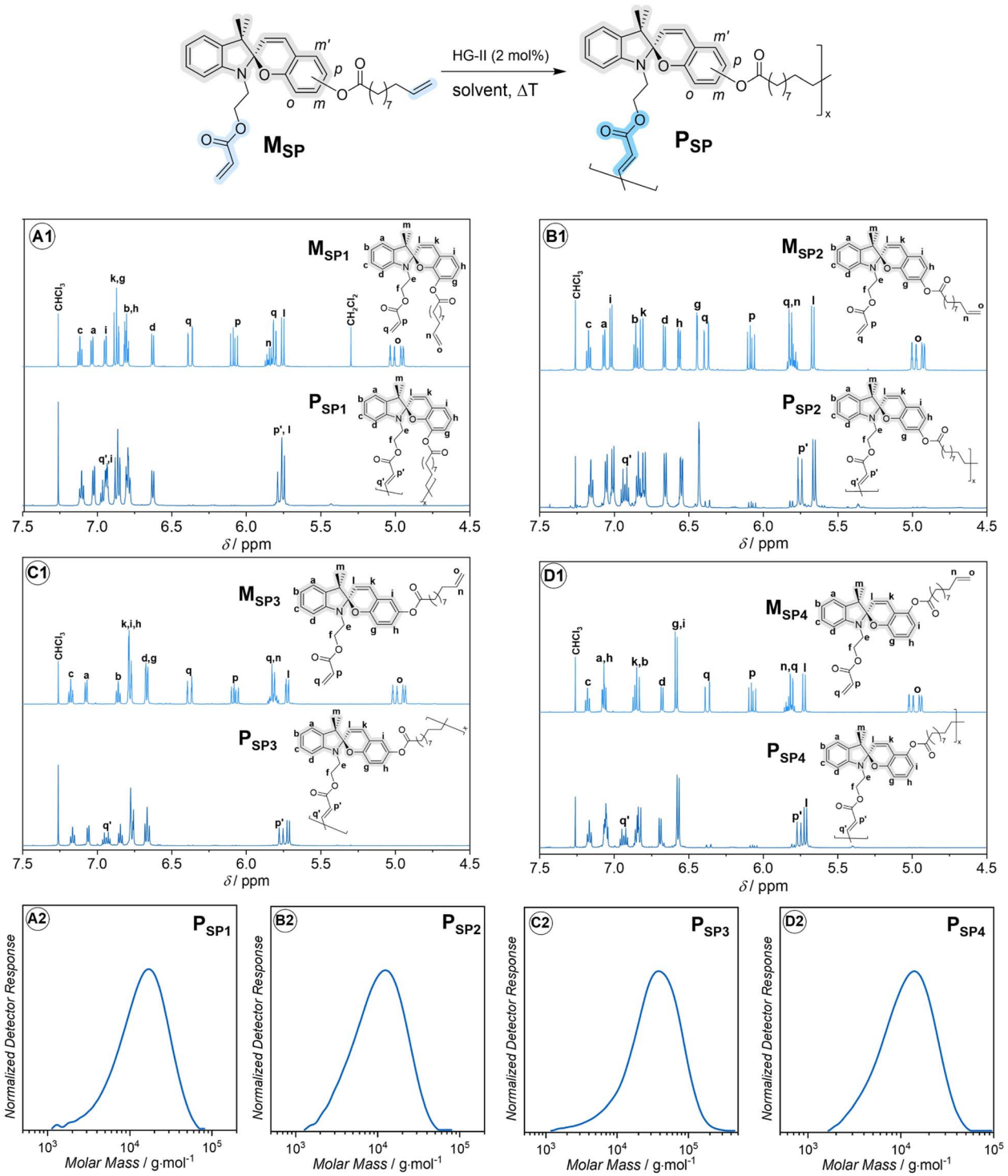

Fig. 2 Synthesis and characterization of main-chain spiropyran-based polymers. Top: synthesis *via* head-to-tail ADMET polymerization and ^{1}H NMR sectional spectra (600 MHz, 32 scans, $CDCl_3$) of monomers and polymers: (A1) $\mathbf{M_{SP1}}$ and $\mathbf{P_{SP1}}$, (B1) $\mathbf{M_{SP2}}$ and $\mathbf{P_{SP2}}$, (C1) $\mathbf{M_{SP3}}$ and $\mathbf{P_{SP3}}$, (D1) $\mathbf{M_{SP4}}$ and $\mathbf{P_{SP4}}$. Full 1D and 2D NMR spectra are provided in the ESI, Section 9.† The assignment of the proton resonances was assisted through the analysis of 1D and 2D NMR spectra of precursors and desired products as described in ESI, Section 9.† Details of the polymerization conditions can be found in the ESI, Section 2.† Bottom: dimethylacetamide (DMAc)-size exclusion chromatography (SEC) traces of $\mathbf{P_{SP1}}$ (A2), $\mathbf{P_{SP2}}$ (B2), $\mathbf{P_{SP3}}$ (C2) and $\mathbf{P_{SP4}}$ (D2).

Table 1).[23] The molar absorptivity of the SP chromophore at λ_{max} (*i.e.*, ε_{max}) for $\mathbf{P_{SP1}}$, $\mathbf{P_{SP2}}$, $\mathbf{P_{SP3}}$ and $\mathbf{P_{SP4}}$ varies between 3700 M^{-1} cm^{-1} and 4700 M^{-1} cm^{-1}, respectively (Table 1).

Fundamentally, the closed- and open-conformation switching of SPs is a complex process, as there are several possible transient states, which have been subjected to careful experimental and

Table 1 Molar mass, dispersity, and optical properties of P_{SP1}, P_{SP2}, P_{SP3} and P_{SP4}

	M_n[a]/g mol^{-1}	M_p[a]/g mol^{-1}	$Đ$[a]	λ_{max}[b]/nm	ε_{max}[b]/M^{-1} cm^{-1}
$\mathbf{P_{SP1}}$	11 000	17 000	1.6	297	4130
$\mathbf{P_{SP2}}$	8000	12 000	1.6	299	4630
$\mathbf{P_{SP3}}$	22 000	39 000	1.9	299	3710
$\mathbf{P_{SP4}}$	7500	10 500	1.5	298	3850

[a] Dimethylacetamide (DMAc)-size exclusion chromatography (SEC), on the basis of poly(methyl methacrylate) (PMMA) calibration. [b] In dichloromethane (DCM) at 25 °C.

theoretical investigation.[39–44] Briefly, the photo-induced transformation of SPs first takes place *via* the cleavage of the labile C–O spiro bond, followed by *E*/*Z*-isomerization around specific bonds (Scheme 1) to form the merocyanine (**MC**) form (opened form).[42] In the presence of a strong acid, the protonation of spiro oxygen and the subsequent isomerization generates thermally stable species (**MCH$^+$**).[42] However, probing the switching mechanism is not the main aim of the current study. Instead, we explore the effect of the molecular design on the switching efficiency of SPs main-chain polymers. Specifically, we reveal the effect of the location of the ester group on the chromene moiety on photo- and halochromism. We exploit the intense color difference between the spiropyran (closed-form, colorless) and the **MC**/**MCH$^+$** form (opened-form, colored), monitored by UV-vis spectroscopy, to compare the photo- and pH-responsive properties among $\mathbf{P_{SP1}}$, $\mathbf{P_{SP2}}$, $\mathbf{P_{SP3}}$ and $\mathbf{P_{SP4}}$, underpinned by careful ^{1}H NMR spectroscopic analysis.

Photochromism

Initially, we conducted the irradiation of the four polymer solutions (50–150 μM) in dichloromethane (DCM) at ambient temperature (25 °C). We selected a wavelength of 330 nm (monochromatic) to minimize unfavorable side reactions, such as photodegradation. The UV-vis spectra in Fig. 3 demonstrate the different photochromism of the investigated polymers. There is almost no vivid color change of the $\mathbf{P_{SP1}}$ polymer solution unless when irradiated with relatively large number of photons (N_p) ($N_p = 6.0 \times 10^{19}$ photons) (Fig. 3A). In contrast, the UV-vis spectra of $\mathbf{P_{SP2}}$, $\mathbf{P_{SP3}}$ and $\mathbf{P_{SP4}}$ display new and strong absorption bands in the visible region (Fig. 3B–D) upon irradiation. It is noticeable in the case of the latter polymers that beside an emerging absorption peak centered at around 458–477 nm, there is an absorption band lying at lower wavelengths close to 380–390 nm, suggesting the existence of at least two isomers of the opened form, *e.g.*, (*Z*)- and (*E*)-isomers of **MC** (Scheme 1). Intriguingly, the color of the $\mathbf{P_{SP1}}$ solution in DCM gradually turned yellow in the dark after long time exposure to 330 nm irradiation ($N_p = 6.0 \times 10^{19}$ photons) (Fig. 3A). We cannot exclude the solvent contributions, *e.g.*, from DCM, to the photochromism of SPs, as frequently reported in the literature.[45–48] Nevertheless, it is worth noting that the pristine polymer solutions in DCM did not show any change in color at 25 °C in the dark, excluding solvatochromism as the root cause of the color change. However, to our surprise, the irradiation performed in other solvents, *i.e.*, toluene and dimethylacetamide (DMAc), did not trigger a noticeable response from all four polymers (UV-vis spectra shown in Fig. S7†). We chose toluene and DMAc alongside DCM as solvents for the irradiation study due to the good solubility of the polymers in these solvents which are of different polarity.

Protic solvents capable of forming H-bonds, such as methanol, can stabilize the merocyanine (**MC**) form, thus facilitating the photo-induced SP → MC conversion process.[48] However, the four SP-based polymers reported in our work are hydrophobic and do not dissolve in such protic solvents. Toluene and DMAc do not possess H-bonding capabilities. In addition, DMAc can act as a Lewis base[49,50] which may react with the opened form of spiropyran induced by Lewis acid addition.[51] However, it is not relevant to our case where no Lewis acid was added in the irradiation study. Even though DCM is not a protic solvent, its role as a very weak H-donor was previously reported,[52] which may be a contributing factor for the color change observed for $\mathbf{P_{SP2}}$, $\mathbf{P_{SP3}}$, $\mathbf{P_{SP4}}$ under 330 nm irradiation in DCM. However, we cannot discard the possibility of UV-induced degradation of the halogenated solvents, *e.g.*, CH_2Cl_2, $CHCl_3$, into halogen acids, *e.g.*, HCl, that can cause the change in color of these polymer solutions owing to the generally acid-sensitive characteristics of SPs. For instance, Sommer and colleagues reported the *in situ* generation of acid from DCM-d_2 and chloroform-*d* under sonication, which was responsible for the chromism of the reported SP-based polymers in the respective solvents.[32,53]

To confirm the possible *in situ* generation of halogen acid under UV-irradiation, we conducted control experiments in which only the blank DCM solvent was irradiated with an exact number of photons previously applied for each SP-based polymer solution, after which the stock polymer solution was rapidly added to the UV-exposed solvent. $\mathbf{P_{SP1}}$ in post-irradiated DCM shows a gradual increase in the visible absorption region (λ_{max} = 439 nm), which is identical with the irradiated $\mathbf{P_{SP1}}$ solution mentioned above (Fig. 3A, E and I). Thus, the acid-induced ring-opening and isomerization observed for $\mathbf{P_{SP1}}$ takes place in the dark after 330 nm irradiation (6.0×10^{19} photons). In the case of $\mathbf{P_{SP2}}$ and $\mathbf{P_{SP3}}$, the HCl formed *in situ* also co-contributes to the color change (compare Fig. 3B, C, F,

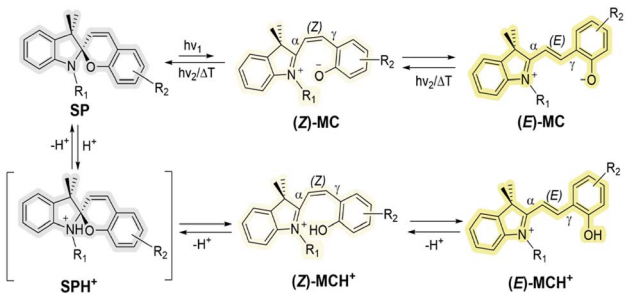

Scheme 1 Simplified mechanism of photo- and acid-induced ring-opening and isomerization of SPs. The (*Z*)-MC/MCH$^+$ and (*E*)-MC/MCH$^+$ can adopt other conformations *via* rotation around the α- and γ-bond. Details of the stimuli-responsive mechanism can be found in ref. 1, 2 and 39–44.

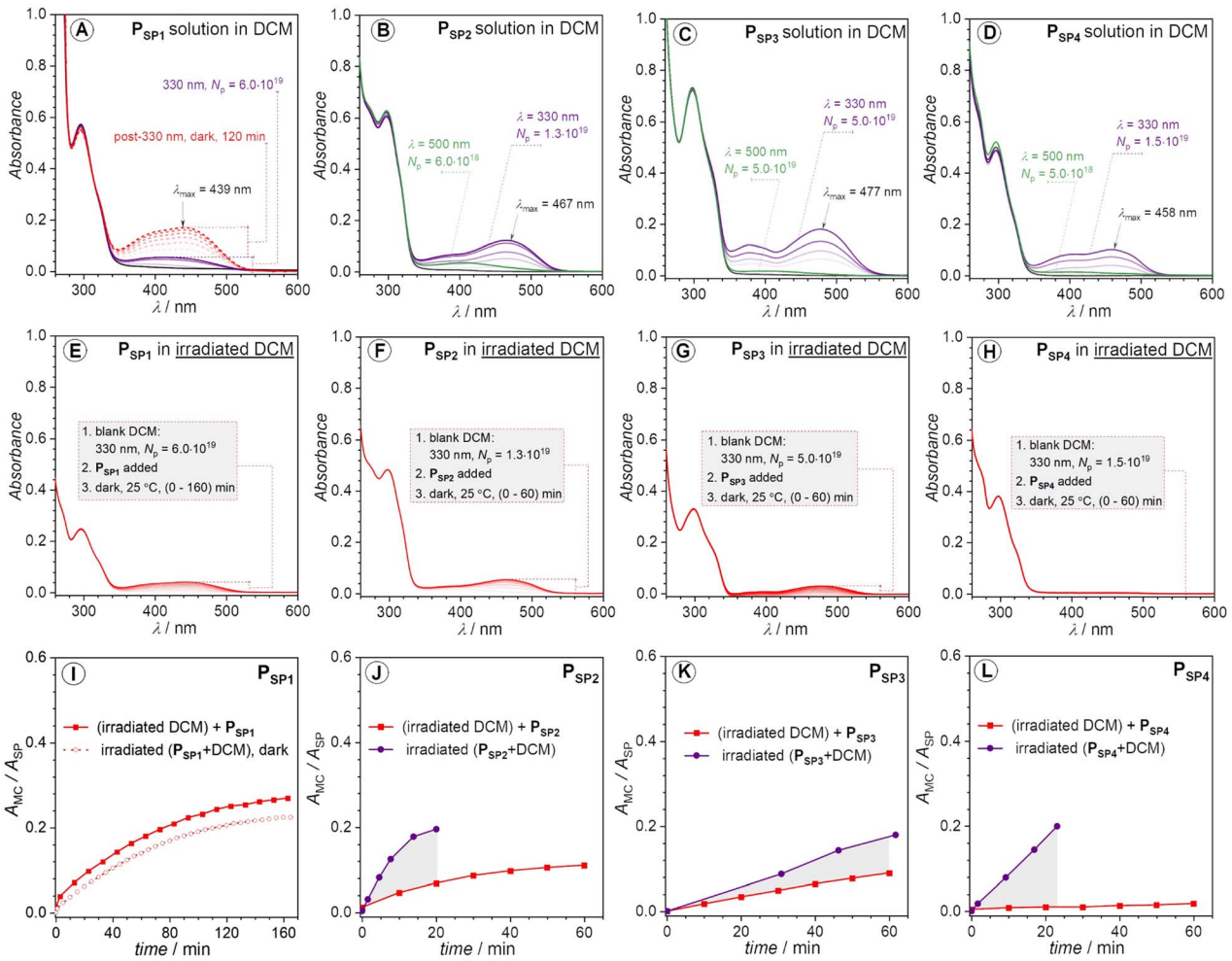

Fig. 3 (A–D) UV-vis spectra of P_{SP1}, P_{SP2}, P_{SP3} and P_{SP4} solution in DCM, recorded before and after 330 nm monochromatic irradiation at 25 °C. The red dashed lines denote the spectra recorded post 330 nm irradiation; the purple solid lines represent the spectra recorded immediately after 330 nm irradiation; the green solid lines indicate the spectra recorded after 500 nm irradiation of the 330 nm irradiated solutions. (E–H) UV-vis spectra recorded upon addition of P_{SP1}, P_{SP2}, P_{SP3} and P_{SP4}, to 330 nm irradiated DCM blank solvents. Molar concentrations were between 50 and 150 μM. Enlargements of UV-vis spectra in (A–H) are available in the ESI, Fig. S8.† The laser power at 330 and 500 nm irradiation was kept at 6.5 mW ± 5.2% and 8.5 mW ± 13%, respectively. (I–L) Plots of A_{MC}/A_{SP} *vs.* time for P_{SP1}, P_{SP2}, P_{SP3} and P_{SP4}, respectively. Note that the protonated form of **MC** (MCH^+) also exists but is grouped into the '**MC**' label in A_{MC} (*i.e.*, absorbance of the opened form) for the sake of simplicity. The absorbance of the '**MC**' label in this case (A_{MC}) corresponds to the λ_{max} of the colored species in the visible range, and the A_{SP} refers to the absorbance at λ_{max} of the respective spiropyran. The A_{MC}/A_{SP} ratio is used instead of A_{MC} to factor in the concentration difference between experiments assuming $A_{MC}/A_{SP} \sim c_{MC}/c_{SP}$ with $\varepsilon_{MC}/\varepsilon_{SP}$ = constant. The number of photons (N_p) was converted into time *via* eqn S1.† The gray areas in (J–L) highlight the actual photochromic response of polymer solutions upon 330 nm irradiation.

G, J and K). However, $\mathbf{P_{SP4}}$ appears to be barely affected in the irradiated blank solvent (Fig. 3D, H and L). Therefore, these results allow to conclude that $\mathbf{P_{SP4}}$ is the most photo-active polymer, while $\mathbf{P_{SP1}}$ is insensitive to solution photo-irradiation. In other words, the substitution site of the ester group on the chromene moiety does indeed critically influence the photochromic properties of the main-chain polymers. It should be noted that the comparison made here is qualitative, yet sufficiently convincing. Based on UV-vis spectra alone (Fig. 3), we cannot quantify the ratio of the opened-form induced by irradiation. However, irradiation of higher concentrated solutions (close to 0.96 mM in DCM-d_2) with 330 nm laser light did not cause any change in the ^{1}H NMR spectra, probably due to the low efficiency of the photo-induced SP → **MC** transformation at higher concentrations (millimolar *vs.* micromolar), also noted by Ballester and colleagues for a similar spiropyran compound.[54]

The colored state of the opened-form can be quenched *via* visible light irradiation (λ = 500 nm, P = 8.5 mW ± 13%) (Fig. 3B–D). However, as can be seen in Fig. 3B–D, while the absorption at around (450–480) nm completely disappears under 500 nm irradiation, the shoulder absorption band close to 390 nm persists. The incomplete visible light-induced colored to colorless reversion may be due to the stabilizing effect from either acidic protons or the solvent (DCM). In addition, we note the contribution of the polymer backbone to

the thermal stability of the opened-form.[55] To avoid the impact from the *in situ* forming acid (HCl), we performed the irradiation in thin films (solid-state) to expand the potential application scope of the polymers on the example of polymer $\mathbf{P_{SP2}}$. Under similar irradiation condition ($\lambda = 330$ nm, $N_p = 1.5 \times 10^{19}$, $P = 6.5$ mW $\pm$ 4.0%), the color of the polymer film on a quartz slide turned yellow, detectable with the naked eye. Indeed, the recorded UV-vis spectrum (Fig. S2†) revealed a new broad absorption band in the visible region (up to 650 nm), suggesting SP $\rightarrow$ **MC** transformation in the solid state. However, the solid-state UV-vis spectrum of the **MC** is vastly different from the solution one, likely due to the intermolecular stacking of the formed **MC** species in the confined environment in the polymer film. Nevertheless, we have demonstrated the feasibility of solid-state photochromism of the SP-based polymer, *i.e.*, $\mathbf{P_{SP2}}$.

Halochromism

The different responses of the polymers to the photogenerated acids indicate the strong effect of the molecular architecture on the halochromism of the main-chain polymers, which we systematically investigated with the addition of two acids with different pK_a (trifluoroacetic acid, CF_3COOH (TFA), p$K_a = 0.23$,[56] methanesulfonic acid, CH_3SO_3H (MsOH), p$K_a = -1.9$)[57] to the polymer solutions in DCM. To avoid the acids affecting the polymer chain, such as cleavage of ester bonds, we added only 1.0 molar equivalent of either TFA or MsOH (with respect to the SP core) to the polymer solutions. The colorimetric response was monitored by UV-vis and ^{1}H NMR spectroscopy. As shown in Fig. 4A–C, the solution of $\mathbf{P_{SP2}}$ swiftly changes color upon TFA addition, reaching an equilibrium within 3 hours. Equilibration of the color changing process took significantly longer for $\mathbf{P_{SP1}}$ and $\mathbf{P_{SP3}}$. The observed color change is due to the formation of $\mathbf{MCH^+}$.[40] In contrast to $\mathbf{P_{SP1}}$, $\mathbf{P_{SP2}}$, and $\mathbf{P_{SP3}}$, the $\mathbf{P_{SP4}}$ solution was hardly affected by TFA addition (Fig. 4D), which is opposite to the strong photochromism of $\mathbf{P_{SP4}}$ discussed above.

Upon the addition of the stronger acid, *i.e.*, MsOH (pK_a = -1.9),[57] the change in absorbance is significantly larger than in the case of TFA addition, except for $\mathbf{P_{SP4}}$ which remains largely unaffected (compare Fig. 4A–D and E–H). The absorption spectra of these $\mathbf{MCH^+}$ species also feature a major absorption band within the 440–465 nm range and a shoulder at around 376–393 nm (Fig. 4), indicating the existence of different stable isomers, *e.g.*, **(*Z*)-** and **(*E*)-MCH$^+$** (Scheme 1). The varied sensitivity towards acids of these polymers is a strong indication of different pK_a values of the respective phenolate anions upon ester substitution of the chromene ring. To compare the kinetics of the halochromic processes for $\mathbf{P_{SP1}}$, $\mathbf{P_{SP2}}$ and $\mathbf{P_{SP3}}$, we qualitatively compared the curvature of the (normalized) absorbance (at λ_{max} of $\mathbf{MCH^+}$) *vs.* time plot (Fig. 4I–N). For both TFA (p$K_a = 0.23$)[56] and MsOH (p$K_a = -1.9$)[57] addition, $\mathbf{P_{SP2}}$ is the most responsive polymer, followed by $\mathbf{P_{SP1}}$ and $\mathbf{P_{SP3}}$ which show slightly different rates of response (Fig. 4I–N).

If one compares the acid-induced and the photo-induced UV-vis spectra of $\mathbf{P_{SP2}}$ and $\mathbf{P_{SP3}}$ in DCM (Fig. 3 and 4), no prominent shift ((3–4) nm) in the peak and shoulder absorption in the visible region can be observed. For nitrospiropyrans, a large spectral shift between the protonated **MC** ($\mathbf{MCH^+}$) and the **MC** form was reported.[58] In the case of our ester-substituted main-chain SPs, the presence of the ester groups might bridge the electronic differences between the **MC** and $\mathbf{MCH^+}$ forms. Alternatively, the H-bonding stabilization from the solvent, *i.e.*, DCM, might equalize the spectral characteristics of the **MC** and $\mathbf{MCH^+}$.

To quantify the ratio of the $\mathbf{MCH^+}$ species in each polymer, we replicated the study using more concentrated solutions (close to 0.97 mM of SP moiety in CD_2Cl_2) for ^{1}H NMR measurements. Accordingly, comparison of the integral values of protons e ($\delta \approx 4.25$ ppm) and f ($\delta \approx 3.25$–3.60 ppm) in the closed-form (as shown in Fig. 2 and S3–S6†) with those in the opened-form gives the percentage of $\mathbf{MCH^+}$ species (Fig. S3–S6†). Approximately 50% of the spiropyran moieties in $\mathbf{P_{SP2}}$ transformed into the opened form ($\mathbf{MCH^+}$) upon addition of TFA (1.0 eq.), twice as high as for $\mathbf{P_{SP3}}$ (25%) under identical conditions (Fig. S4 and S5†). Similar to $\mathbf{P_{SP3}}$, the determined value for $\mathbf{P_{SP1}}$ is 29%, whereas only 9% was recorded for $\mathbf{P_{SP4}}$ (Fig. S1 and S6†). The relative amount of $\mathbf{MCH^+}$ increases further when MsOH is added instead: close to 75% of $\mathbf{MCH^+}$ for $\mathbf{P_{SP1}}$, $\mathbf{P_{SP2}}$ and $\mathbf{P_{SP3}}$ and only 10% for $\mathbf{P_{SP4}}$ (Fig. S3–S6†). Interestingly, although the former polymers show the same ratio of $\mathbf{MCH^+}$ species induced by MsOH addition at equilibrium, the absorbance or molar absorptivity of the $\mathbf{MCH^+}$ in the case of $\mathbf{P_{SP2}}$ appears to be much higher than $\mathbf{P_{SP1}}$ and $\mathbf{P_{SP3}}$. Thus, the ester-substitution pattern affects not only the acid sensitivity of SPs, but also the molar absorptivity of the resulting $\mathbf{MCH^+}$. In addition, the highly polar nature of $\mathbf{MCH^+}$ can lead to aggregation in solution at high conversion,[59] as indicated by Dynamic Light Scattering (DLS) results for the MsOH-added polymer solutions (Fig. S1†). Further, addition of 2.0 eq. of triethyl amine (Et_3N) fully reverted the $\mathbf{MCH^+}$ to the closed-form, as evidenced by ^{1}H NMR spectroscopy (Fig. S3–S6†).

The experimental results discussed above clearly point to the significant role of the ester group substituted on the chromene ring beside the contribution from the solvent polarity. Since the chromene ring directly attaches to the oxygen of the ester (–**O**COR), the ester group serves as a moderate electron-donating group (EDG), directing electrons to the *ortho*- and *para*-position (relative to that EDG) of the phenyl ring. However, the same phenyl ring is at the same time substituted with two other groups, *i.e.*, the spiro oxygen (in the closed-form) or the phenolate oxygen (in the opened-form) and the ethene bridge (–C=CR″, R″ contains the indoline moiety), which are also EDGs. Thus, there are three EDGs on the phenyl ring under discussion (Scheme 2). Depending on their relative positions on the ring, the electron density of the phenolate oxygen (O^-) (forming upon ring-opening) may be different. During the photochromism of SPs, we hypothesize that the merocyanine form is more stable when electrons on the phenolate oxygen are directed to the ring or elsewhere (*i.e.*, lower electron density on the O^- group).[60] In $\mathbf{P_{SP4}}$ – which is the most photoresponsive polymer – the O^- and the ester groups are *meta*-substituted to each other, but *ortho*-substituted to the ethene bridge (Scheme 2), thus facilitating the synergistic pushing of electrons from these two groups to

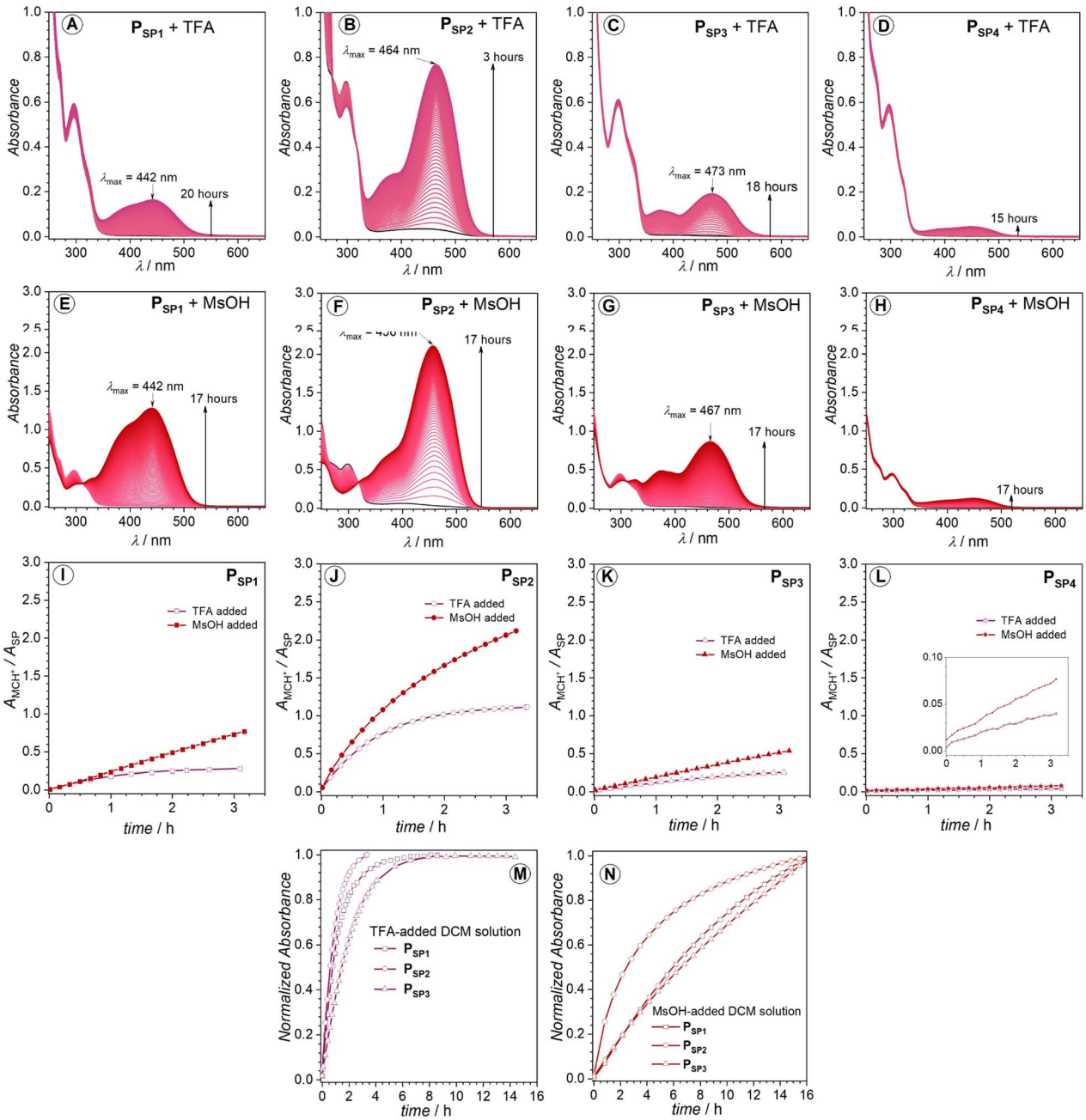

Fig. 4 Halochromism of $\mathbf{P_{SP1}}$, $\mathbf{P_{SP2}}$, $\mathbf{P_{SP3}}$, $\mathbf{P_{SP4}}$ in DCM from UV-vis spectroscopy. (A–D) TFA addition (1.0 eq.), (E–H) MsOH addition (1.0 eq.). Time until equilibration is indicated. Molar concentration of SP moiety: 100–150 μM. (I–N) Comparison of the kinetics among four polymers upon acid addition. Normalized absorbance was used in (M and N) to enable a qualitative comparison of the response rate of the polymers toward TFA and MsOH acid. The A_{MCH^+}/A_{SP} ratio is used instead of A_{MCH^+} to factor in the concentration difference between experiments assuming $A_{MCH^+}/A_{SP} \sim c_{MCH^+}/c_{SP}$ with $\varepsilon_{MCH^+}/\varepsilon_{SP} =$ constant. A_{MCH^+} refers to the absorbance (A) of the $\mathbf{MCH^+}$ form at λ_{max} in the visible range, and A_{SP} refers to the absorbance of the pristine SP at λ_{max}.

the ethene bridge, effectively reducing the electron density on the O^- group. On the basis of this logic and in consideration of the steric hindrance at the *o*-position, the poor photochromic property observed for $\mathbf{P_{SP1}}$ can be explained (Scheme 2). Meanwhile, a less electron density in the phenolate oxygen also suggests a less susceptibility to protonation, agreeing well with the experimental result for $\mathbf{P_{SP4}}$, which is the most acid-resistant among the four polymers studied. In the same manner, $\mathbf{P_{SP1}}$ is supposed to be the most acid-sensitive. Nevertheless, $\mathbf{P_{SP2}}$ surpasses $\mathbf{P_{SP1}}$ in terms of halochromism. Close inspection of the $\mathbf{P_{SP2}}$ structure suggests possible hydrogen bonding of the phenolate O^- and the carbonyl oxygen (of the ester) to the proton from acids and DCM solvent (Scheme 2), perhaps making $\mathbf{P_{SP2}}$ more sensitive towards acids than $\mathbf{P_{SP1}}$. In addition, the substitution of the ester group at the *p*-position with respect to the ethene bridge – where *E*/*Z* isomerization takes

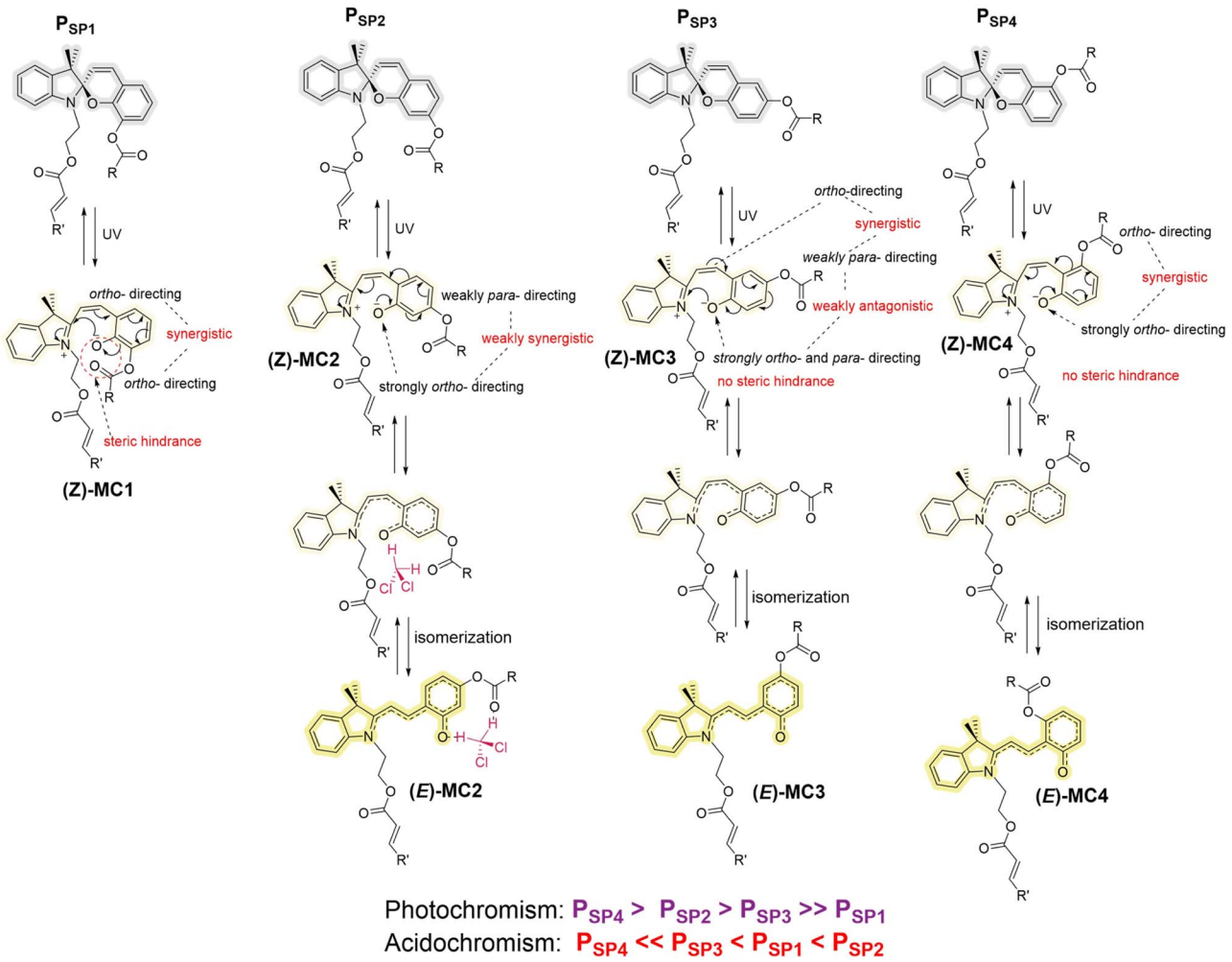

Scheme 2 Possible impacts of the ester group substituted at one of the four possible positions on the chromene moiety (*o*-, *m*-, *p*- and *m*′-, with respect to the benzopyran oxygen) on the stability of the opened-form of spiropyran, impacting the photo- and halochromism. We hypothesize that the resulting photo- and halochromism of the four polymers in DCM solutions originate from a complex combination of electronic effects (induction and resonance), steric hindrance and hydrogen-bonding capability caused by the regio-substitution of the ester (–**O**COR) group. The relative orientation of the phenolate (O^-)/phenolic (OH) oxygen, the ethene bridge and the ester group (which are all electron-donating groups (EDGs)) may influence the electron densities on these groups. In the case of P_{SP1} and P_{SP3}, for instance, both the ethene bridge and the ester groups are at either *ortho*-/*ortho*- or *ortho*-/*para*-positions with respect to the phenolate oxygen and *vice versa*. Thus, the former groups can synergistically direct electrons to the phenolate oxygen. There exists also a possibility for the phenolate oxygen (which is a much stronger EDG) to redirect electron density to the other two groups. For P_{SP1}, the steric contribution from the ester group and the possible electronic repulsion between the phenolate oxygen (O^-) and the carbonyl oxygen in the ester group may further reduce the photochromic response of the polymer compared to P_{SP3}. However, upon protonation, a possible hydrogen bonding between these two groups can be established, co-contributing to the strong halochromism of P_{SP1}. In the case of P_{SP2} and P_{SP4}, the phenolate oxygen is *meta*-substituted with respect to the ester group. Thus, these two EDGs can cooperatively push electron density to the ethene bridge, leading to lower electron densities on the phenolate oxygen (which means stronger photochromism). With regard to the observed halochromism, P_{SP2} and P_{SP4} are expected to be inactive or significantly less responsive compared to P_{SP1} and P_{SP3}. However, while the prediction holds true for P_{SP4}, P_{SP2} responds fastest to acid-addition. Upon careful structural analysis, we submit that the possible intermolecular interaction with the solvent (DCM), *i.e.*, hydrogen-bonding, and the geometry of the ester group (which also functions as the connecting arm) beside the electronic contribution, lead to the unexpected performance of P_{SP2}. Within all four polymers, the ester group in P_{SP2} is at the *para*-position with respect to the ethene bridge, where *E*/*Z*-isomerization takes place upon ring-opening. In terms of steric hindrance, such a substitution site is the most ideal and thus does not interfere with the *E*/*Z*-isomerization at the ethene bridge. The term "*ortho*-directing" refers to the electron-donation from the substituent under consideration to its *ortho*-position.

place upon ring-opening in $\mathbf{P_{SP2}}$ – is the most ideal among all four polymers in terms of steric hindrance, facilitating the isomerization process in $\mathbf{P_{SP2}}$. Nevertheless, an in-depth theoretical study, which is out of scope of this work, is required to fully understand the role of such ester substituents (–**O**COR).

Furthermore – since the phenolate O^- group is a much stronger EDG than the ester group – the substitution of the ester group at *ortho*- and *para*-position respective to the O^- group – as seen in $\mathbf{P_{SP1}}$ and $\mathbf{P_{SP3}}$ – might make the ester group function as an electron-receiving group. As a result, the carbonyl oxygen of

the ester might become more prone to protonation, leading to cleavage of the ester group. Indeed, the Size Exclusion Chromatography (SEC) traces recorded for $\mathbf{P_{SP1}}$ and $\mathbf{P_{SP3}}$ (Fig. S3 and S5†) show a drastic reduction in M_n upon addition of the strong acid, *i.e.*, MsOH, whereas $\mathbf{P_{SP2}}$ and especially $\mathbf{P_{SP4}}$ stay relatively unaffected under the same conditions. The ^{1}H NMR spectra (Fig. S3 and S5†) of $\mathbf{P_{SP1}}$ and $\mathbf{P_{SP3}}$ solutions upon addition of MsOH followed by quenching with Et_3N also indicate some degree of degradation. Since the chromophore and the acrylate C=C bonds remain intact upon quenching with Et_3N, the degradation (if applicable) is highly likely due to the hydrolysis of the main-chain ester group on the chromene moiety. Polymer chains generally break in the middle of the chain owing to entropic reason, which leads to a large shift in the apparent molar mass despite only a minor degree of hydrolysis.[61] The FT-IR spectrum of MsOH-added $\mathbf{P_{SP3}}$ – which showed the largest shift in the SEC – suggests only little ester hydrolysis (Fig. S9†). Thus, in addition to the inherit photo- and acidochromism of SPs, the position of the ester group (–**O**COR) on the chromene moiety of SPs may complementarily affect its hydrolysis induced by acids.

Conclusions

We herein introduce the synthesis of main-chain polymers derived from four regional isomers ($\mathbf{P_{SP1}}$, $\mathbf{P_{SP2}}$, $\mathbf{P_{SP3}}$ and $\mathbf{P_{SP4}}$) of spiropyrans *via* head-to-tail ADMET polymerization. The photo- and halochromism of these polymers are highly dependent on the position of the ester group (–**O**COR) on the phenyl ring of the chromene, which is essential to incorporate the stimuli responsive spiropyrans in the main chain. While $\mathbf{P_{SP4}}$ (ester group (–**O**COR) in the *m*′-position) responds fastest under UV irradiation, no pronounced response is observed under acidic conditions (addition of 1.0 eq. of CF_3COOH (TFA) or CH_3SO_3H (MsOH)). In contrast, $\mathbf{P_{SP1}}$ (ester group (–**O**COR) in the *o*-position) reacts relatively fast to an acid stimulus, yet at the same time is inactive towards UV exposure. Both $\mathbf{P_{SP2}}$ and $\mathbf{P_{SP3}}$ (ester group (–**O**COR) at *m*-position and *p*-position, respectively) are responsive toward irradiation and acids. These characteristics are clearly attributed to the change in the substitution site of the ester group on the benzopyran (chromene) moiety. The herein discussed findings thus allow to manipulate and fine-tune the properties of stimuli responsive spiropyran-based main-chain polymers for specific applications, requiring limited synthetic effort. We anticipate the influence of substitution extends towards other stimuli such as metal ions and force. Critically, our results demonstrate the significance of small isomeric molecular variations in conjunction with transitioning from side-chain decorated to main-chain based macromolecular architectures, including their potential for finely modulating the characteristics of stimuli responsive polymeric materials.

Data availability

All experimental data and detailed experimental procedures are available in the main text and ESI.†

Author contributions

L. D. T. conceptualized the spiropyran system, conducted all experimental work and wrote the initial draft of the manuscript. J. A. K. assisted with data interpretation and discussion and co-edited the manuscript. C. B.-K. and H. M. motivated and conceptualized the research direction, acquired funding, discussed the data and edited the manuscript.

Conflicts of interest

The authors declare no conflicts of interests.

Acknowledgements

C. B.-K. acknowledges the Australian Research Council (ARC) for funding in the context of a Laureate Fellowship enabling his photochemical research program. The authors acknowledge funding for the project from QUT's Centre for Materials Science. The Central Analytical Research Facility (CARF) at QUT is gratefully acknowledged. H. M. acknowledges the University of Haute-Alsace (UHA) for the financial support from the French National Research Agency (ANR) with the reference "ANR-22-CPJ1-0077-01" and from the CNRS for a junior professorship contract. C. B.-K. acknowledges additional funding by the Deutsche Forschungsgemeinschaft (DFG, German Research Foundation) under Germany's Excellence Strategy for the Excellence Cluster '3D Matter Made to Order' (EXC-2082/1 – 390761711). J. A. K. acknowledges the Deutsche Forschungsgemeinschaft (DFG, German Research Foundation) for his WBP fellowship – 500289223.

References

1 R. Klajn, Spiropyran-based dynamic materials, *Chem. Soc. Rev.*, 2014, **43**, 148–184.
2 L. Kortekaas and W. R. Browne, The evolution of spiropyran: fundamentals and progress of an extraordinarily versatile photochrome, *Chem. Soc. Rev.*, 2019, **48**, 3406–3424.
3 J. K. Rad, Z. Balzade and A. R. Mahdavian, Spiropyran-based advanced photoswitchable materials: a fascinating pathway to the future stimuli-responsive devices, *J. Photochem. Photobiol., C*, 2022, **51**, 100487.
4 M. Li, Q. Zhang, Y.-N. Zhou and S. Zhu, Let spiropyran help polymers feel force!, *Prog. Polym. Sci.*, 2018, **79**, 26–39.
5 H. Decker and H. Felser, Über cyclische Oxoniumsalze aus Dicumarketon und über Spiropyranderivate, *Ber. Dtsch. Chem. Ges.*, 1908, **41**, 2997–3007.
6 L. Florea, D. Diamond and F. Benito-Lopez, Photo-responsive polymeric structures based on spiropyran, *Macromol. Mater. Eng.*, 2012, **297**, 1148–1159.
7 M. Sommer, Substituent effects control spiropyran–merocyanine equilibria and mechanochromic utility, *Macromol. Rapid Commun.*, 2021, **42**, 2000597.
8 B. Di Credico, G. Griffini, M. Levi and S. Turri, Microencapsulation of a UV-responsive photochromic dye by means of novel UV-screening polyurea-based shells for

smart coating applications, *ACS Appl. Mater. Interfaces*, 2013, **5**, 6628–6634.

9 L. Kortekaas, O. Ivashenko, J. T. van Herpt and W. R. Browne, A remarkable multitasking double spiropyran: bidirectional visible-light switching of polymer-coated surfaces with dual redox and proton gating, *J. Am. Chem. Soc.*, 2016, **138**, 1301–1312.

10 F. Jiang, S. Chen, Z. Cao and G. Wang, A photo, temperature, and pH responsive spiropyran-functionalized polymer: synthesis, self-assembly and controlled release, *Polymer*, 2016, **83**, 85–91.

11 Y. Lin, M. H. Barbee, C.-C. Chang and S. L. Craig, Regiochemical effects on mechanophore activation in bulk materials, *J. Am. Chem. Soc.*, 2018, **140**, 15969–15975.

12 F. Arjmand and Z. Mohamadnia, Fabrication of a light-responsive polymer nanocomposite containing spiropyran as a sensor for reversible recognition of metal ions, *Polym. Chem.*, 2022, **13**, 937–945.

13 Y. Vidavsky, S. J. Yang, B. A. Abel, I. Agami, C. E. Diesendruck, G. W. Coates and M. N. Silberstein, Enabling room-temperature mechanochromic activation in a glassy polymer: synthesis and characterization of spiropyran polycarbonate, *J. Am. Chem. Soc.*, 2019, **141**, 10060–10067.

14 A. Fagan, M. Bartkowski and S. Giordani, Spiropyran-based drug delivery systems, *Front. Chem.*, 2021, **9**, 720087.

15 Y. Jung, H. Lee, T.-J. Park, S. Kim and S. Kwon, Programmable gradational micropatterning of functional materials using maskless lithography controlling absorption, *Sci. Rep.*, 2015, **5**, 15629.

16 H. Vijayamohanan, E. F. Palermo and C. K. Ullal, Spirothiopyran-based reversibly saturable photoresist, *Chem. Mater.*, 2017, **29**, 4754–4760.

17 G. Stoychev, A. Kirillova and L. Ionov, Light-responsive shape-changing polymers, *Adv. Opt. Mater.*, 2019, **7**, 1900067.

18 G. D. Jaycox, Stimuli-responsive polymers. VIII. Polyesters and poly (ester amides) containing azobenzene and chiral binaphthylene segments: highly adaptive materials endowed with light-, heat-, and solvent-regulated optical rotatory power, *J. Polym. Sci., Part A: Polym. Chem.*, 2006, **44**, 207–218.

19 L. D. Thai, T. R. Guimaraes, S. Spann, A. S. Goldmann, D. Golberg, H. Mutlu and C. Barner-Kowollik, Photoswitchable block copolymers based on main chain α-bisimines, *Polym. Chem.*, 2022, **13**, 5625–5635.

20 P. Min, Y. Li, L. Wang, W. Song and L. Ding, The shackling photoisomerization effect on self-assembly of azobenzene-containing side-chain homopolymers, *Polymer*, 2022, **258**, 125301.

21 M. Wei, Y. Gao, X. Li and M. J. Serpe, Stimuli-responsive polymers and their applications, *Polym. Chem.*, 2017, **8**, 127–143.

22 P. Schattling, F. D. Jochum and P. Theato, Multi-stimuli responsive polymers–the all-in-one talents, *Polym. Chem.*, 2014, **5**, 25–36.

23 M. Schulz-Senft, P. J. Gates, F. D. Sönnichsen and A. Staubitz, Diversely halogenated spiropyrans-Useful synthetic building blocks for a versatile class of molecular switches, *Dyes Pigm.*, 2017, **136**, 292–301.

24 H. Görner, Photochromism of nitrospiropyrans: effects of structure, solvent and temperature, *Phys. Chem. Chem. Phys.*, 2001, **3**, 416–423.

25 J. H. Day, Thermochromism, *Chem. Rev.*, 1963, **63**, 65–80.

26 F. Kempe, L. Metzler, O. Brügner, H. Buchheit, M. Walter, H. Komber and M. Sommer, Substituent-controlled energetics and barriers of mechanochromic spiropyran-functionalized poly (ε-caprolactone), *Macromol. Chem. Phys.*, 2023, **224**, 2200254.

27 A. Kellmann, F. Tfibel, E. Pottier, R. Guglielmetti, A. Samat and M. Rajzmann, Effect of nitro substituents on the photochromism of some spiro [indoline-naphthopyrans] under laser excitation, *J. Photochem. Photobiol., A*, 1993, **76**, 77–82.

28 M. Sakuragi, K. Aoki, T. Tamaki and K. Ichimura, The role of triplet state of nitrospiropyran in their photochromic reaction, *Bull. Chem. Soc. Jpn.*, 1990, **63**, 74–79.

29 S. Bhattacharyya, M. Maity, A. Chowdhury, M. L. Saha, S. K. Panja, P. J. Stang and P. S. Mukherjee, Coordination-assisted reversible photoswitching of spiropyran-based platinum macrocycles, *Inorg. Chem.*, 2020, **59**, 2083–2091.

30 A. S. Kozlenko, A. D. Pugachev, I. V. Ozhogin, I. M. El-Sewify and B. S. Lukyanov, Spiropyrans: molecules in motion, *Chem. Heterocycl. Compd.*, 2021, **57**, 984–989.

31 G. R. Gossweiler, T. B. Kouznetsova and S. L. Craig, Force-rate characterization of two spiropyran-based molecular force probes, *J. Am. Chem. Soc.*, 2015, **137**, 6148–6151.

32 M. Sommer and H. Komber, Spiropyran main-chain conjugated polymers, *Macromol. Rapid Commun.*, 2013, **34**, 57–62.

33 C. K. Lee, D. A. Davis, S. R. White, J. S. Moore, N. R. Sottos and P. V. Braun, Force-induced redistribution of a chemical equilibrium, *J. Am. Chem. Soc.*, 2010, **132**, 16107–16111.

34 V. Pantsyrnyi and M. Gal'bershtam, Preparation of spiropyrans from 3-formylsalicylic acid derivatives, *Chem. Heterocycl. Compd.*, 1971, **7**, 134–135.

35 L. D. Thai, T. R. Guimaraes, L. C. Chambers, J. A. Kammerer, D. Golberg, H. Mutlu and C. Barner-Kowollik, Molecular photoswitching of main-chain α-bisimines in solid-state polymers, *J. Am. Chem. Soc.*, 2023, **145**, 14748–14755.

36 L. Ding, Y. Li, H. Cang, J. Li, C. Wang and W. Song, Controlled synthesis of azobenzene-containing block copolymers both in the main-and side-chain from SET-LRP polymers *via* ADMET polymerization, *Polymer*, 2020, **190**, 122229.

37 S. Mavila, C. E. Diesendruck, S. Linde, L. Amir, R. Shikler and N. G. Lemcoff, Polycyclooctadiene complexes of rhodium (I): direct access to organometallic nanoparticles, *Angew. Chem., Int. Ed.*, 2013, **22**, 5767–5770.

38 L. D. Thai, J. Fanelli, R. Munaweera, M. O'Mara, C. Barner-Kowollik and H. Mutlu, Main-chain macromolecular

hydrazone photoswitches, *Angew. Chem., Int. Ed. Engl.*, 2023, e202315887.

39 V. I. Minkin, Photo-, thermo-, solvato-, and electrochromic spiroheterocyclic compounds, *Chem. Rev.*, 2004, **104**, 2751–2776.

40 J. T. Wojtyk, A. Wasey, N.-N. Xiao, P. M. Kazmaier, S. Hoz, C. Yu, R. P. Lemieux and E. Buncel, Elucidating the mechanisms of acidochromic spiropyran-merocyanine interconversion, *J. Phys. Chem. A*, 2007, **111**, 2511–2516.

41 R. Ganesan and F. Remacle, Stabilization of merocyanine by protonation, charge, and external electric fields and effects on the isomerization of spiropyran: a computational study, *Theoretical Chemistry in Belgium: A Topical Collection from Theoretical Chemistry Accounts*, 2014, pp. 167–179.

42 L. Kortekaas, J. Chen, D. Jacquemin and W. Browne, Proton-stabilized photochemically reversible E/Z isomerization of spiropyrans, *J. Phys. Chem. B*, 2018, **122**, 6423–6430.

43 S.-R. Keum, K.-B. Lee, P. M. Kazmaier and E. Buncel, A novel method for measurement of the merocyanine-spiropyran interconversion in non-activated 1,3,3-trimethylspiro-(2*H*-1-benzopyran-2,2′-indoline) derivatives, *Tetrahedron Lett.*, 1994, **35**, 1015–1018.

44 H. Shiozaki, Molecular orbital calculations for acid induced ring opening reaction of spiropyran, *Dyes Pigm.*, 1997, **33**, 229–237.

45 N. A. Murugan, S. Chakrabarti and H. Ågren, Solvent dependence of structure, charge distribution, and absorption spectrum in the photochromic merocyanine–spiropyran pair, *J. Phys. Chem. B*, 2011, **115**, 4025–4032.

46 J. Piard, Influence of the solvent on the thermal back reaction of one spiropyran, *J. Chem. Educ.*, 2014, **91**, 2105–2111.

47 W. Tian and J. Tian, An insight into the solvent effect on photo-, solvato-chromism of spiropyran through the perspective of intermolecular interactions, *Dyes Pigm.*, 2014, **105**, 66–74.

48 S. Weber, Stabilization of the merocyanine form of photochromic compounds in fluoro alcohols is due to a hydrogen bond, *Chem. Commun.*, 1998, 2685–2686.

49 J.-J. Zhang, X.-H. Duan, Y. Wu, J.-C. Yang and L.-N. Guo, Transition-metal free C–C bond cleavage/borylation of cycloketone oxime esters, *Chem. Sci.*, 2019, **10**, 161–166.

50 Y. Li, K. Cheng, X. Lu and J. Sun, A Facile and Efficient Approach to N-Protected-β-Sulfinyl-enamines *via* C-Sulfinylation of Enamides and Enecarbamates, *Adv. Synth. Catal.*, 2010, **352**, 1876–1880.

51 K. Guo and Y. Chen, Lewis acid and base triggered molecular switch, *J. Mater. Chem.*, 2009, **19**, 5790–5793.

52 A. Allerhand and P. Von Rague Schleyer, A survey of CH groups as proton donors in hydrogen bonding, *J. Am. Chem. Soc.*, 1963, **85**, 1715–1723.

53 H. Komber, S. Müllers, F. Lombeck, A. Held, M. Walter and M. Sommer, Soluble and stable alternating main-chain merocyanine copolymers through quantitative spiropyran–merocyanine conversion, *Polym. Chem.*, 2014, **5**, 443–453.

54 P. Ferreira, G. Moncelsi, G. Aragay and P. Ballester, Hydrogen-bonded dimeric capsules with appended spiropyran units: towards controlled cargo release, *Chem.–Eur. J.*, 2021, **27**, 12675–12685.

55 E. Goldburt, F. Shvartsman, S. Fishman and V. Krongauz, Intramolecular interactions in photochromic spiropyran-merocyanine polymers, *Macromolecules*, 1984, **17**, 1225–1230.

56 D. R. Lide, *CRC Handbook of Chemistry and Physics*, CRC Press, 2004.

57 J. P. Guthrie, Hydrolysis of esters of oxy acids: pKa values for strong acids; Brønsted relationship for attack of water at methyl; free energies of hydrolysis of esters of oxy acids; and a linear relationship between free energy of hydrolysis and pKa holding over a range of 20 p K units, *Can. J. Chem.*, 1978, **56**, 2342–2354.

58 M. E. Genovese, E. Colusso, M. Colombo, A. Martucci, A. Athanassiou and D. Fragouli, Acidochromic fibrous polymer composites for rapid gas detection, *J. Mater. Chem. A*, 2017, **5**, 339–348.

59 Y. Onai, M. Mamiya, T. Kiyokawa, K. Okuwa, M. Kobayashi, H. Shinohara and H. Sato, Colored merocyanine aggregates: long-lived crystals of large size (10-100 mu m) and deaggregation of small aggregates in solutions, *J. Phys. Chem.*, 1993, **97**, 9499–9505.

60 T. Satoh, K. Sumaru, T. Takagi, K. Takai and T. Kanamori, Isomerization of spirobenzopyrans bearing electron-donating and electron-withdrawing groups in acidic aqueous solutions, *Phys. Chem. Chem. Phys.*, 2011, **13**, 7322–7329.

61 K. Pahnke, J. Brandt, G. Gryn'Ova, C. Y. Lin, O. Altintas, F. G. Schmidt, A. Lederer, M. L. Coote and C. Barner-Kowollik, Entropy-driven selectivity for chain scission: where macromolecules cleave, *Angew. Chem., Int. Ed.*, 2016, **55**, 1514–1518.